

## Supporting Information

# The effect of heteroatoms at end groups of anthracene derivatives on the photoelectric properties and crystal/film morphology: a theoretical perspective

Gui-Ya Qin,<sup>a</sup> Xiao-Qi Sun,<sup>b</sup> Pan-Pan Lin,<sup>a,c</sup> Xue Wei,<sup>a</sup> Jing-Fu Guo,<sup>b</sup> Wei-Bo Cui,<sup>a</sup> Jian-Xun Fan,<sup>d</sup> Hui Li,<sup>a</sup> Lu-yi Zou,<sup>a</sup> and Ai-min Ren<sup>\*a</sup>

*a. College of Chemistry, Jilin University, Changchun, 130023, China*

*b. School of Physics, Northeast Normal University, Changchun 130024, P.R. China*

*c. College of Chemistry and Chemical Engineering, Qiqihar University, Qiqihar, 161006, P.R. China.*

*d. College of Chemistry and Materials Science, Weinan Normal University, Weinan 714000, China.*

Corresponding Authors: Ai-min Ren

**E-mail:** [renam@jlu.edu.cn](mailto:renam@jlu.edu.cn)

## Part 1: Selection of Calculation Method

For small organic molecules and solid systems, the most commonly used functionals to calculate the basic electronic structural properties are PBE0 (25% Hartree–Fock exchange) and B3LYP (20% Hartree–Fock exchange). The B3LYP and PBE0 are recognized as hybrid functional with higher accuracy and affordable computation cost. In order to avoid ignoring other more suitable functional, we used different functionals (B3LYP, PBE0, M062X, wb97xd, CAM-B3LYP functionals) and different basis sets (6-31g(d), 6-31g(d,p), 6-31+g(d,p)) to test the charge transport and luminescence properties of studied systems. Considering the charge transport and luminescence properties are measured in the thin-film environment, the ONIOM model is considered to simulate the solid phase environment.

According to the HOMO/LUMO measured in experiment, we found that the B3LYP/6-31+g(d,p) and PBE0/6-31+g(d,p) method are the closer to the experimental measurement. Moreover, examining the effect of different basis sets on the calculated molecular structure revealed that the structures are largely unchanged. Based on the above information, finally, the B3LYP/6-31+g(d,p) level was selected to calculate their charge transport property.

**Table S1** Calculation results of frontier molecular orbitals (HOMO/LUMO) for different functionals and basis sets. (Unit: eV)

	B3LYP/6-31g(d)			B3LYP/6-31g(d,p)			B3LYP/6-31+g(d,p)			EXP.		
	HOMO	LUMO	Gap	HOMO	LUMO	Gap	HOMO	LUMO	Gap	HOMO	LUMO	Gap
$\alpha$ - BEPAnt	-4.99	-1.77	3.23	-5.00	-1.78	3.23	-5.26	-2.07	3.19			
$\beta$ - BEPAnt	-5.03	-1.81	3.22	-5.04	-1.82	3.22	-5.30	-2.12	3.18	-5.49	-2.77	2.72
BOPAnt	-4.85	-1.69	3.16	-4.86	-1.70	3.16	-5.13	-2.01	3.12	-5.45	-2.76	2.69
BSPAnt	-4.97	-1.85	3.12	-4.98	-1.86	3.12	-5.22	-2.15	3.07	-5.60	-2.72	2.88
	PBE0/6-31g(d)			PBE0/6-31g(d,p)			PBE0/6-31+g(d,p)					
	HOMO	LUMO	Gap	HOMO	LUMO	Gap	HOMO	LUMO	Gap			
$\alpha$ - BEPAnt	-5.24	-1.71	3.53	-5.25	-1.71	3.53	-5.45	-1.95	3.5			
$\beta$ - BEPAnt	-5.28	-1.75	3.52	-5.28	-1.76	3.52	-5.49	-2.00	3.49			
BOPAnt	-5.10	-1.63	3.47	-5.10	-1.64	3.46	-5.32	-1.89	3.43			
BSPAnt	-5.21	-1.79	3.42	-5.22	-1.80	3.42	-5.4	-2.03	3.37			

As for luminescence property, the spectral properties are easily influenced by different functionals. We tested the effect of different functionals on absorption and emission wavelengths and quantum yields of studied systems. Firstly, according to the maximum absorption wavelength measured experimentally, we narrow down the functional scope initially.

**Table S2** Calculated absorption wavelength under different computational functionals and 6-31g(d,p) basis set and the value of experimental measurement. (Unit: nm)

	B3LYP	PBE0	M06-2X	wB97XD	CAM-B3LYP	EXP.-abs(max)
$\alpha$ -BEPAnt	422.15	409.53	367.50	363.67	369.15	
$\beta$ -BEPAnt	423.71	410.89	368.35	364.28	369.85	400~450 nm
BOPAnt	432.30	418.38	372.59	367.50	373.79	
BSPAnt	437.72	422.78	373.82	367.25	373.98	

From the table above, it can be found that B3LYP or PBE0 functionals combined with 6-31g(d,p) is suitable for the absorption transition property. Since the exact emission wavelength was not given in the experiment, only the blue fluorescence range (400-480nm, DOI: 10.1039/D1CC01145F) was mentioned. With this criterion, the calculation results by PBE0/6-31g(d,p) are considered to better describe the emission property of these molecules.

**Table S3** Calculated emission wavelength under BLYP/PBE0/6-31g(d,p) and the value of experimental measurement. (Unit: nm)

	B3LYP	PBE0	EXP.-ems
$\alpha$ -BEPAnt	479.52	464	blue-fluorescence 400-480 nm
$\beta$ -BEPAnt	--	--	
BOPAnt	487.94	472	(DOI: 10.1039/D1CC01145F)
BSPAnt	491.44	475	

## Part 2 Supplementary Data

**Table S4** The molecular planarity parameter (MPP), span of deviation from plane (SDP) and maximal positive/negative deviation to the fitted plane for studied molecules.

Ground state	MPP/Å	SDP/Å	Maximal-positive/Å	Maximal-negative/Å
$\alpha$ -BEPAnt	0.123	0.417	0.208	-0.208
$\beta$ -BEPAnt	0.136	0.435	0.217	-0.218
BOPAnt	0.153	0.554	0.277	-0.277
BSPAnt	0.159	0.541	0.271	-0.271
S1 state	MPP/Å	SDP/Å	Maximal-positive/Å	Maximal-negative/Å
$\alpha$ -BEPAnt	0.179	0.852	0.426	-0.426
$\beta$ -BEPAnt	--	--	--	--
BOPAnt	0.153	0.489	0.244	-0.245
BSPAnt	0.187	0.805	0.402	-0.403

**Table S5** The relative positions of different dimers in BEPAnt, BOPAnt and BSPAnt crystals.

		R/Å	angle	d <sub>long-axis</sub> /Å	d <sub>short-axis</sub> /Å	d <sub>face-to-face</sub> /Å
BEPAnt	1	4.901	48.09°	--	--	--
	2	4.901	48.09°	--	--	--
	3	6.043	--	0.818	5.459	2.462
BOPAnt +	1	4.830	43.710	--	--	--
	2	4.830	43.710	--	--	--
	3	6.163	--	0.791	5.666	2.294
BSPAnt	1	4.881	45.656°	--	--	--
	2	4.890	45.656°	--	--	--
	3	6.034	--	1.187	5.440	2.337

**Table S6** Parameters of hole transport for studied structures.

	$\lambda_h/\text{meV}$	$r/\text{\AA}$	Hole		$\mu_h\text{-1D-60}^\circ\text{C}$
			$V_h(\text{meV})$	Rate $\text{k-60}^\circ\text{C}$	
<b><math>\alpha</math>-BEPAnt</b>	151.69	4.901	38.32	6.6026521368E+13	2.90
		4.901	38.32	6.6026521368E+13	2.90
		6.043	20.50	1.8896228772E+13	1.19
<b><math>\beta</math>-BEPAnt</b>	148.70	4.901	38.32	6.9397571897E+13	2.94
		4.901	38.32	6.9397571897E+13	2.94
		6.043	20.50	1.9860994759E+13	1.28
<b>BOPAnt</b>	206.51	4.830	33.73	2.5732034920E+13	1.11
		4.830	33.73	2.5732034920E+13	1.11
		6.163	10.90	2.6871656890E+12	0.18
<b>BSPAnt</b>	149.90	4.881	18.17	9.8659713979E+12	0.40
		4.890	17.61	9.2672037034E+12	0.40
		6.034	3.13	2.9276467433E+11	0.02

**Table S7 Theoretically and optimized and experimental cell parameters for these studied structures.**

		Exp.		Theo.			
<b>BEPAnt</b>	Space group	P21/c		P21/c( $\alpha$ -)		P21( $\beta$ -)	
	Unit cell dimensions	a=22.66 $\text{\AA}$	$\alpha=90^\circ$	a=22.662 $\text{\AA}$	$\alpha=90^\circ$	a=6.0426 $\text{\AA}$	$\alpha=90^\circ$
		b=7.72 $\text{\AA}$	$\beta=92.45^\circ$	b=7.7188 $\text{\AA}$	$\beta=92.479^\circ$	b=7.7188 $\text{\AA}$	$\beta=92.479^\circ$
		c=6.04 $\text{\AA}$	$\gamma=90^\circ$	c=6.0426 $\text{\AA}$	$\gamma=90^\circ$	c=22.662 $\text{\AA}$	$\gamma=90^\circ$
	Z	2		2		2	
	Volume	1056.00 $\text{\AA}^3$		1056 $\text{\AA}^3$		1056 $\text{\AA}^3$	
<b>BOPAnt</b>	Space group	Pbca		Pbca			
	Unit cell dimensions	a=7.44 $\text{\AA}$	$\alpha=90^\circ$	a=7.4376 $\text{\AA}$	$\alpha=90^\circ$		
		b=6.16 $\text{\AA}$	$\beta=90^\circ$	b=6.1629 $\text{\AA}$	$\beta=90^\circ$		
		c=42.30 $\text{\AA}$	$\gamma=90^\circ$	c=42.296 $\text{\AA}$	$\gamma=90^\circ$		
	Z	4		4			

	Volume	1938.71 Å <sup>3</sup>		1938.71 Å <sup>3</sup>	
<b>BSPAnt</b>	Space group	P-1		P-1	
	Unit cell dimensions	a=6.03 Å	α=92.83°	a=6.0345 Å	α=92.827°
		b=7.68 Å	β=96.55°	b=7.6843 Å	β=96.554°
		c=22.61 Å	γ=90.10°	c=22.6054 Å	γ=90.103°
	Z	2		2	
	Volume	1040.09 Å <sup>3</sup>		1040.09 Å <sup>3</sup>	

**Table S8** The parameters of morphology predictions for BOPAnt and BSPAnt by means of AE model ( $\{h k l\}$ : the Miller index of the growth facet. Multiplicity: symmetry multiplicity of the facets.  $d_{hkl}$ : interplanar distance. %of Total Facet Area: the percentage of the total habit surface area occupied by all symmetry images of the facet. ).

#### BOPAnt

MI index $\{h k l\}$	Multiplicity	$d_{hkl}$ (Å)	%of Total Facet Area	$E_{att}$ (KJ/mol)	Rate ratio
$\{0 0 2\}, \{0 0 -2\}$	2	21.148	76.6588	-17.3582 ( $E_{vdW}$ :-15.5471 $E_{ele}$ :-1.81117)	1
$\{1 0 2\}, \{1 0 -2\}$ $\{-1 0 -2\}, \{-1 0 2\}$	4	7.016	10.3133	-96.3327 ( $E_{vdW}$ :-81.9669 $E_{ele}$ :-14.3658)	5.55
$\{1 1 1\}, \{-1 1 1\}$ $\{1 -1 1\}, \{1 1 -1\}$ $\{-1 -1\}, \{-1 1 -1\}$ $\{1 -1 -1\}, \{-1 -1 -1\}$	8	4.716	13.0279	-137.7602 ( $E_{vdW}$ :-113.7600 $E_{ele}$ :-24.5408)	7.94

#### BSPAnt

MI index $\{h k l\}$	Multiplicity	$d_{hkl}$ (Å)	%of Total Facet Area	$E_{att}$ (KJ/mol)	Rate ratio
$\{0 0 1\}, \{0 0 -1\}$	2	22.430	81.3283	-6.2630 ( $E_{vdW}$ :-6.03774 $E_{ele}$ :-0.2252)	1
$\{0 1 0\}, \{0 -1 0\}$	2	7.675	10.1466	-42.7393 ( $E_{vdW}$ :-36.5608 $E_{ele}$ :-6.17852)	6.82

{1 0 -1}, {-1 0 1}	2	5.964	5.0130	-67.5263 (E <sub>vdw</sub> :--55.1873 E <sub>ele</sub> :-12.3390)	10.78
{1 1 -1}, {-1 1 1}	2	4.723	1.7243	-70.5454 (E <sub>vdw</sub> :--58.1596 E <sub>ele</sub> :-12.3859)	11.26
{1 -1 -1}, {-1 -1 1}	2	4.700	1.7877	-69.8655 (E <sub>vdw</sub> :--57.4584 E <sub>ele</sub> :-12.4071)	11.16

**Table S9** Electronic emission transitions of BEPAnt, BOPAnt and BSPAnt, calculated at the S<sub>1</sub> optimized geometry by TDDFT in QM/MM ONIOM. (ONIOM(PBE0/6-31g(d,p):uff).

	Excited States	Energy (eV)	QMMM(PBE0)		Major contribution
			Wavelength (nm)	<i>f</i>	
<b>BEPAnt</b>	S1	2.6718	464.05	0.2889	H->L (0.99)
<b>BOPAnt</b>	S1	2.6296	471.50	0.3106	H->L (0.99)
<b>BSPAnt</b>	S1	2.6113	474.80	0.4795	H->L (0.99)

**Table S10** Electronic absorption transitions of BEPAnt, BOPAnt and BSPAnt, calculated at the S<sub>0</sub><sup>opt</sup> optimized geometry by TDDFT in QM/MM.

	Excited States	QMMM(PBE0)		<i>f</i>	Major contribution
		Energy (eV)	Wavelength (nm)		
<b>BEPAnt</b>	S1	3.0275	409.53	0.2920	H->L (0.98)
	S2	3.5142	352.80	0.0025	H-1->L(0.54)
					H->L+1(0.44)
	S3	4.0186	308.52	0.0000	H-2->L(0.79)
					H->L+2(0.19)
S4	4.1453	299.10	2.6844	H-1->L(0.43) H->L+1(0.52)	

<b>BOPAnt</b>	S1	2.9634	418.38	0.3168	H->L (0.98)
	S2	3.4976	354.48	0.0039	H-2->L (0.57)
					H->L+1 (0.39)
	S3	3.7957	326.64	0.0000	H-1->L(0.93)
H->L+2(0.05)					
S4	4.0613	305.28	2.3363	H-3->L(0.03)	
				H-2->L(0.40)	
				H->L+1(0.54)	
<b>BSPAnt</b>	S1	2.9326	422.78	0.4758	H->L (0.99)
	S2	3.4281	361.68	0.0173	H-3->L(0.03)
					H-2->L(0.63)
					H->L+1(0.31)
S3	3.5861	345.74	0.0000	H-1->L(0.95)	
				H->L+2(0.03)	
S4	3.8574	321.42	1.8928	H-3->L(0.07)	
				H-2->L(0.35)	
				H->L+1(0.56)	

---

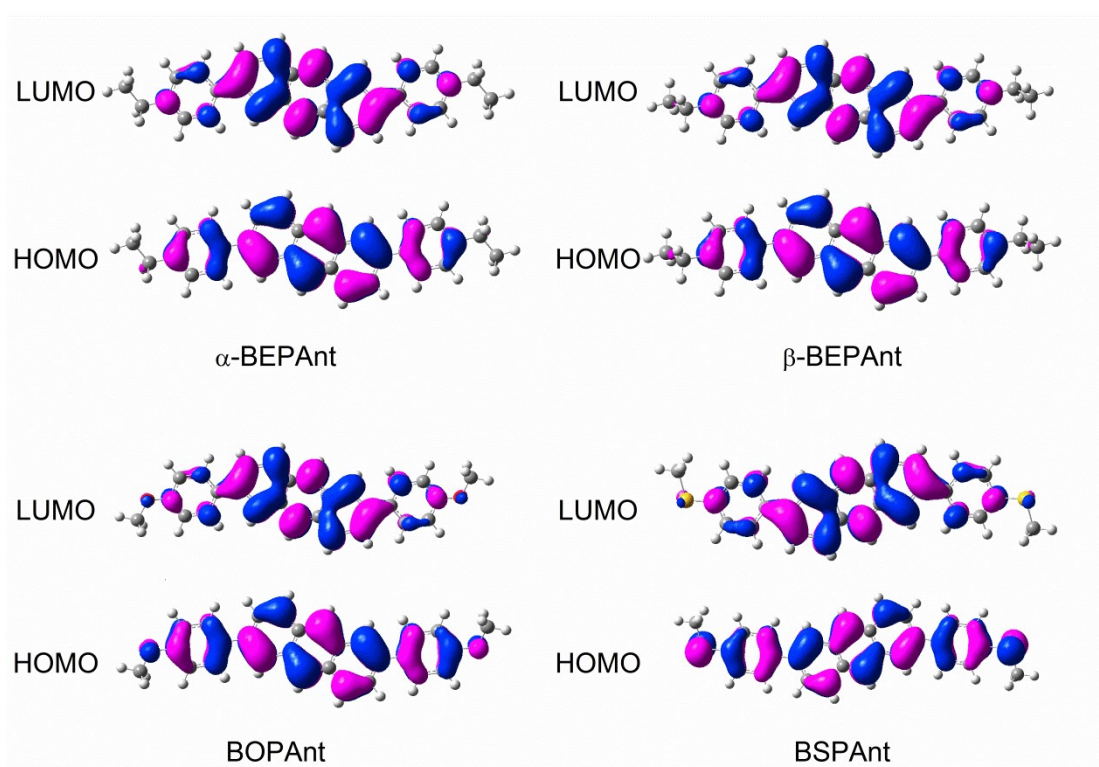


**Figure S1** The frontier molecular orbitals for BEPant, BOPant and BSPant.

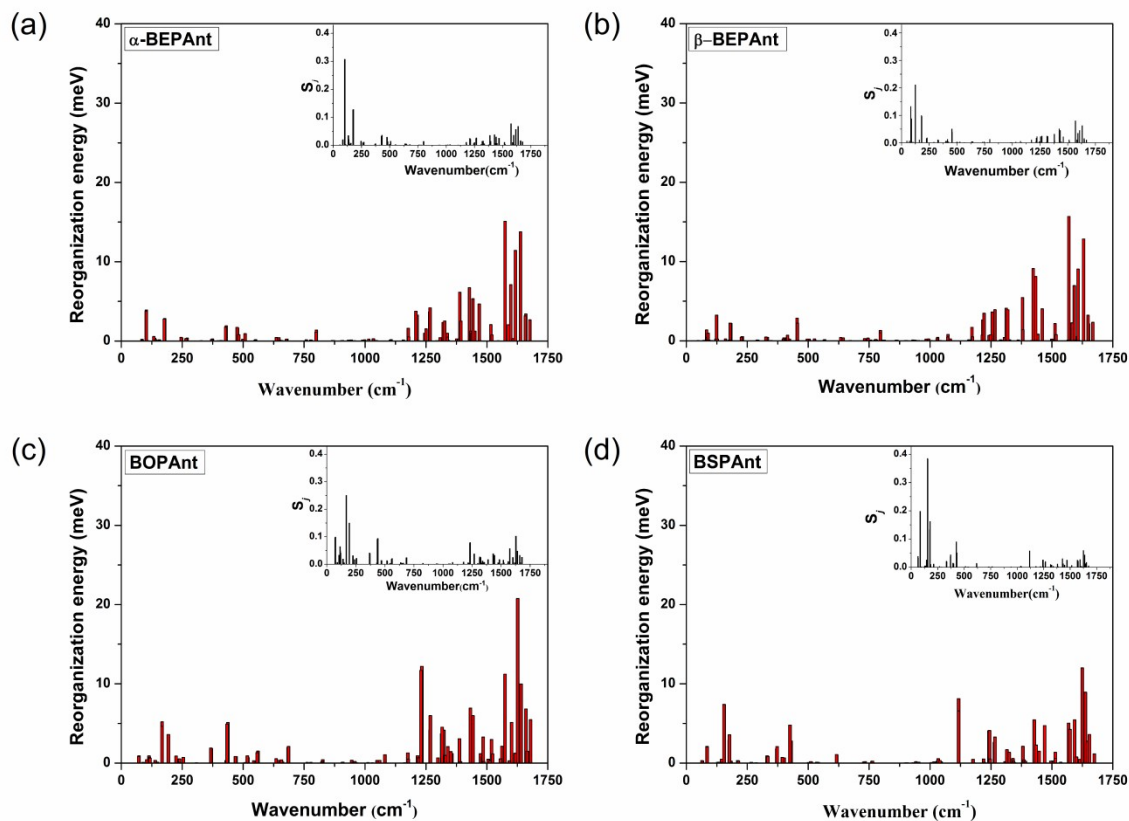


**Figure S2** The contributions of vibration to reorganization energies at the frequency range from 0 cm<sup>-1</sup> to 1750 cm<sup>-1</sup>.

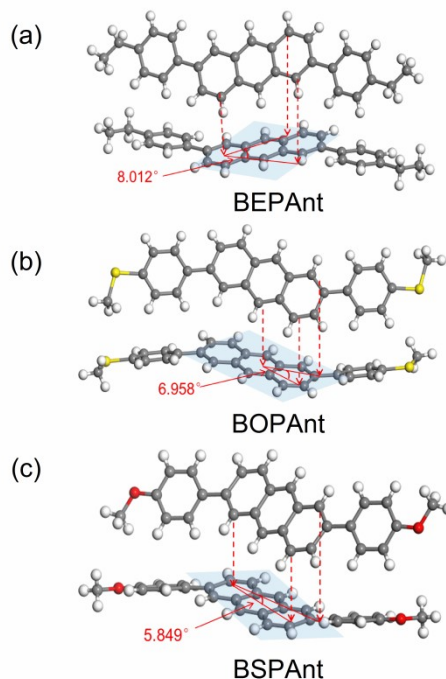


**Figure S3** The projection angle of a dimer in which one molecular skeleton is projected onto the other molecular skeleton.

(NOTE: This method is not universal, because the three crystals are packed in the same way, and the projection of the three selected C atoms in the upper molecule in the figure is in the anthracene skeleton

plane of the lower molecule, so this method can be used for comparison.)

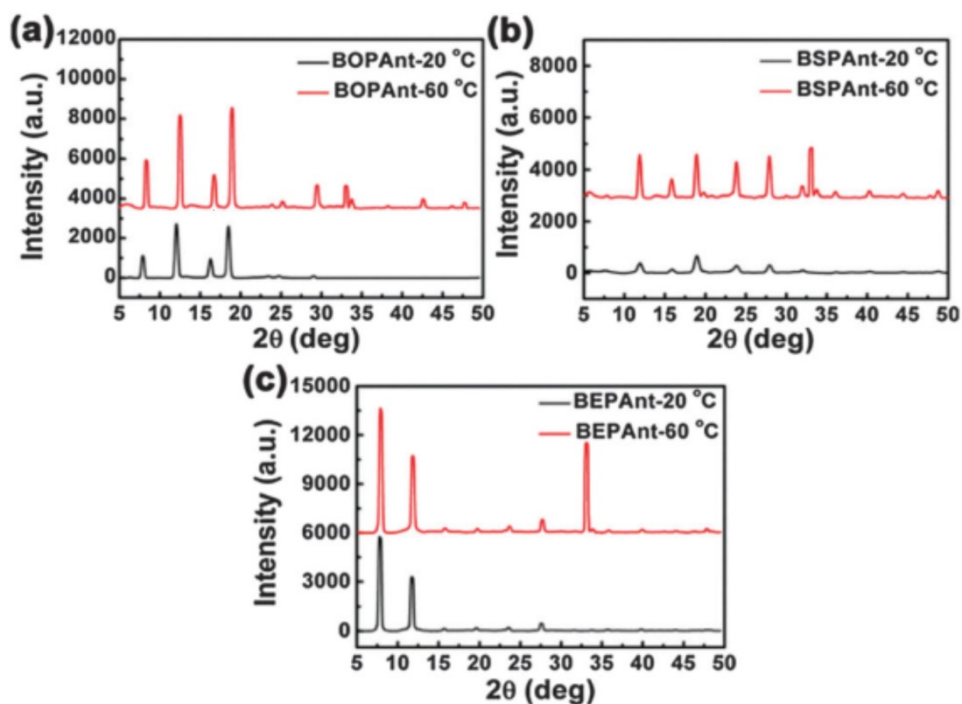


**Figure S4** XRD of the thin films ((a) BOPAnt, (b) BSPAnt, and (c) BEPAnt) deposited at 20 °C (black peaks) and at 60 °C (red peaks) in experiment.<sup>1</sup>

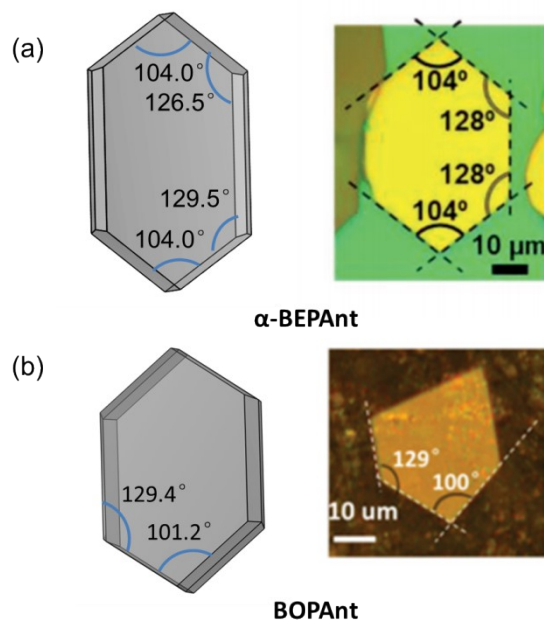


**Figure S5** The predicted morphology (left side) and measured morphology in experiment (right side) of  $\alpha$ -BEPAnt<sup>2</sup> and BOPAnt<sup>3</sup>.

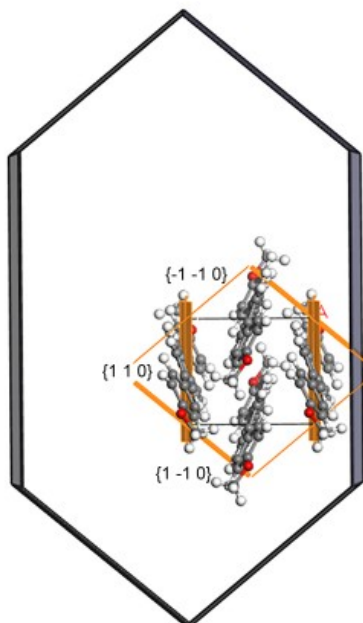


**Figure S6** The MI index facets of the predicted morphology (gray) and measured morphology in experiment (orange) of BOPAnt.<sup>2</sup>

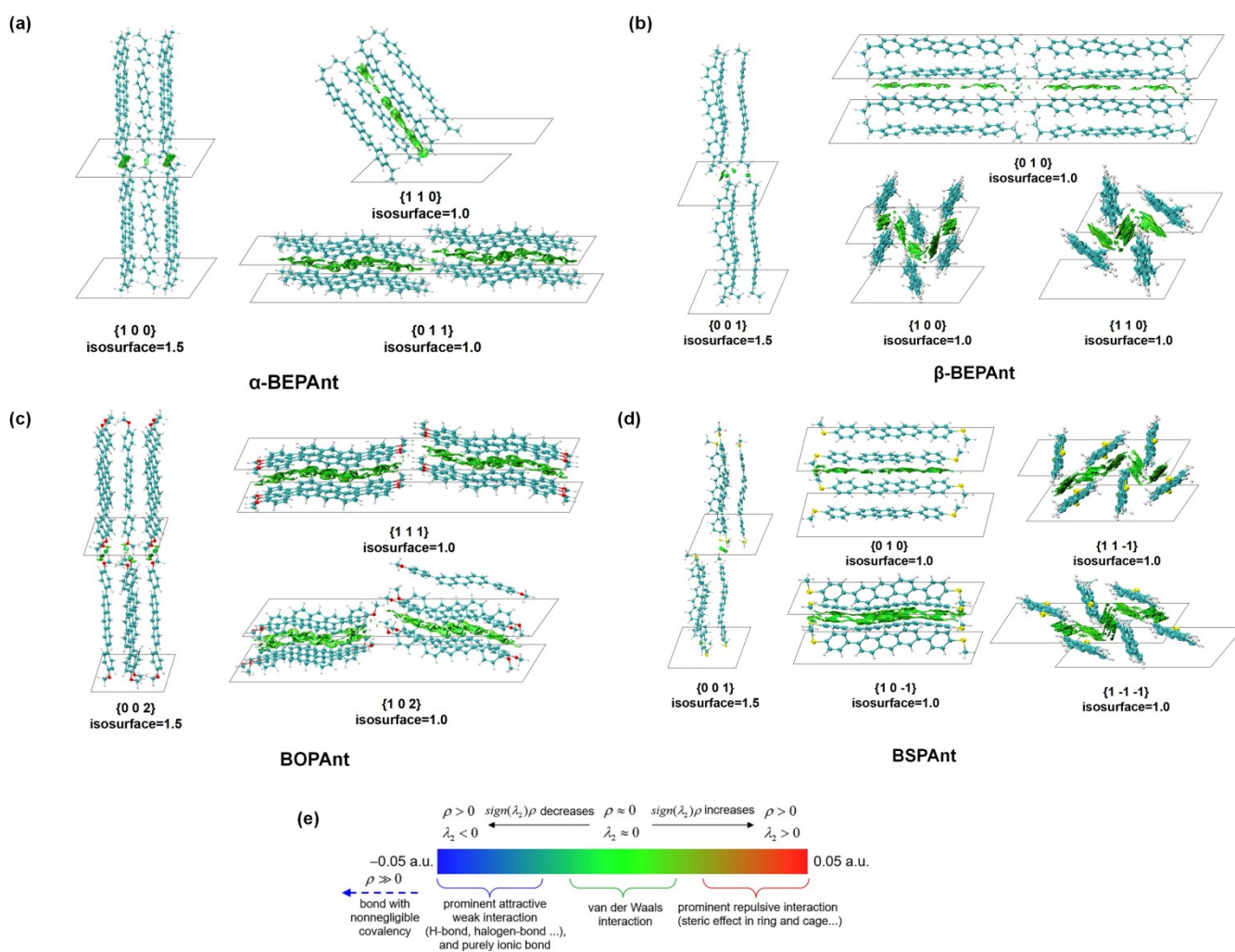


**Figure S7** Isosurface map of IRI for each growth facet of four systems. Isovalue of IRI is chosen to be 1.0 or 1.5. B3LYP-D3(BJ)/6-31g(d,p) level was employed in the calculation and standard coloring method and chemical explanation of  $\text{sign}(\lambda_2)\rho$  on IRI isosurfaces (e).

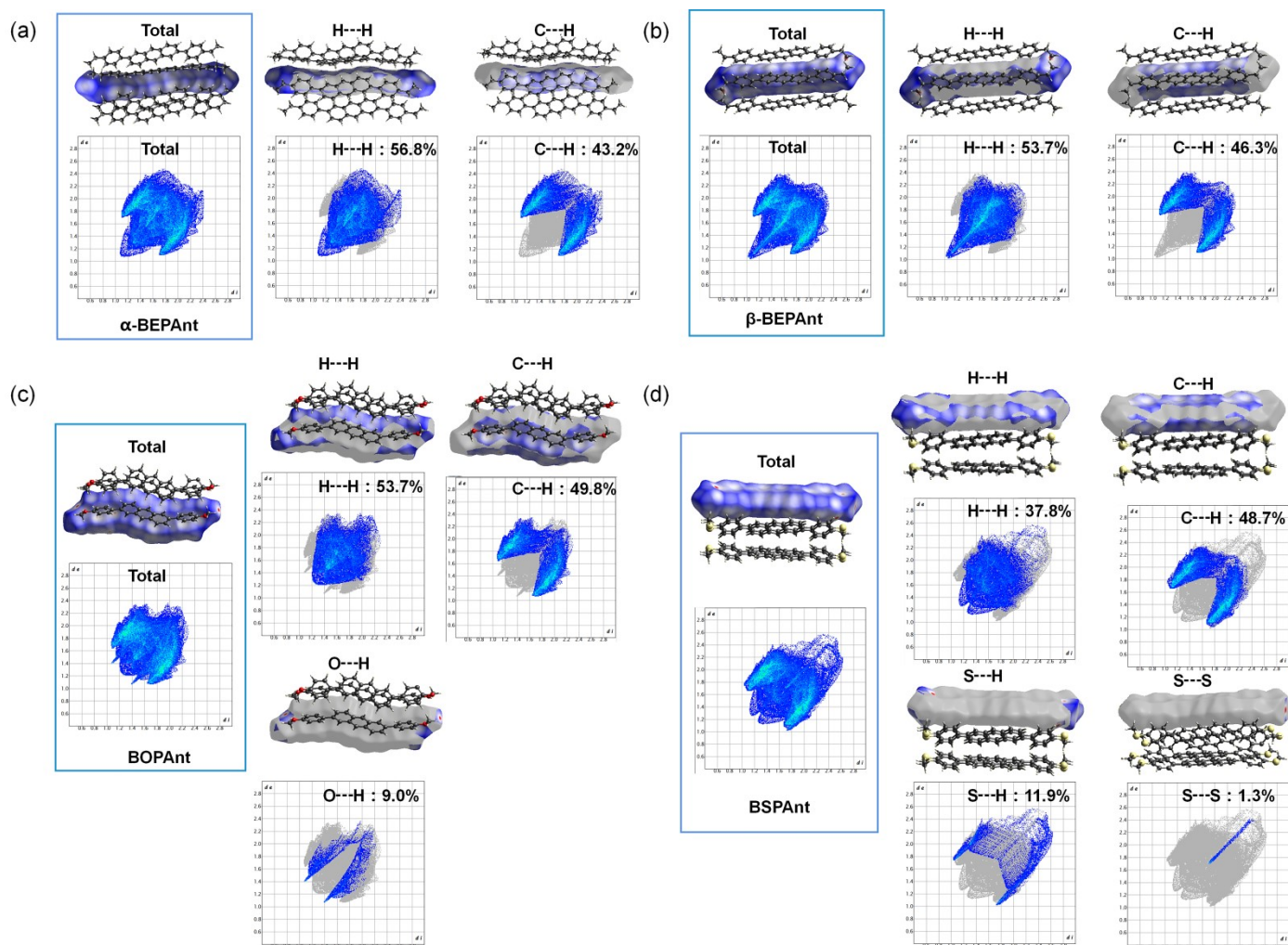


**Figure S8** Hirshfeld surfaces and decomposed fingerprint plots with close contact for  $\alpha$ -BEPant (a),  $\beta$ -BEPant (b), BOPant (c) and BSPant.

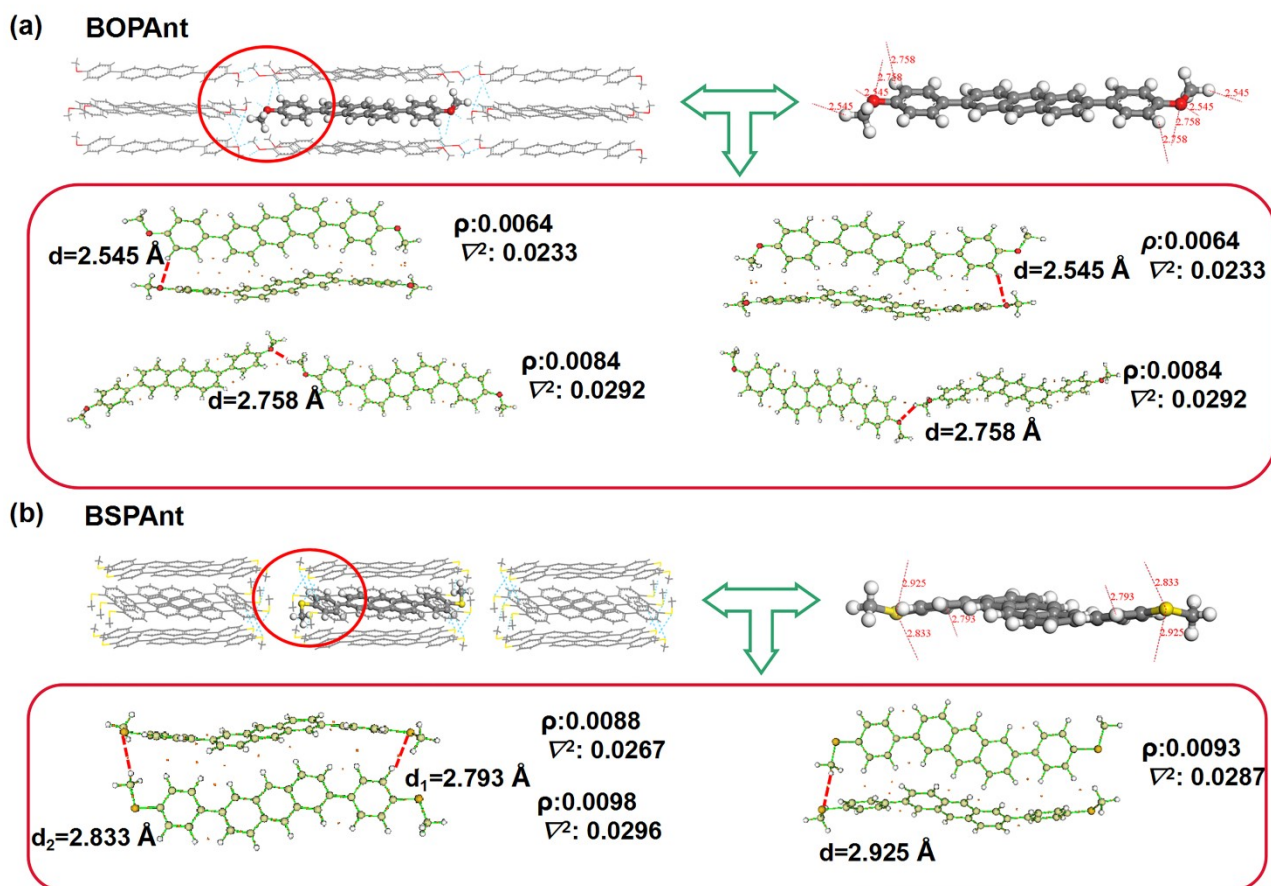


**Figure S9** The major C-H $\cdots$ O and C-H $\cdots$ S hydrogen bonds in BOPAnt and BSPAnt crystal (a) and (b).

Topological properties at the intermolecular C-H $\cdots$ O and C-H $\cdots$ S bond critical points.

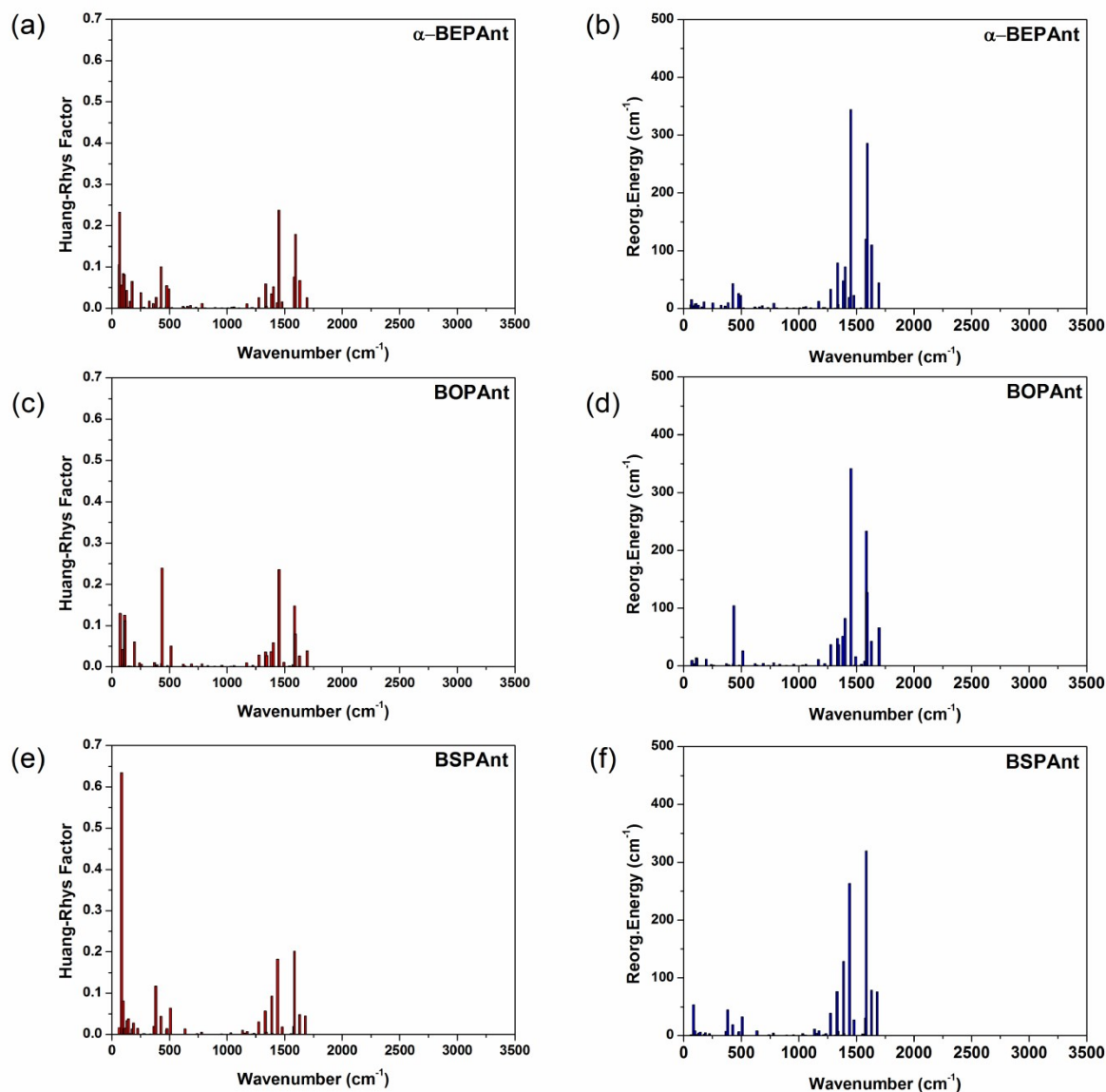


**Figure S10** The contributions of vibrations to reorganization energy and Huang–Rhys factor between  $S_0$  and  $S_1$  states.

## Reference

- [1] L. Yan, Y. Zhao, H. Yu, Z. Hu, Y. He, A. Li, O. Goto, C. Yan, T. Chen, R. Chen, Y.-L. Loo, D. F. Perepichka, H. Meng and W. Huang, *Journal of Materials Chemistry C*, 2016, **4**, 3517-3522.
- [2] C. He, A. Li, L. Yan, D. Zhang, Y. Zhu, H. Chen, H. Meng, O. Goto, 2D and 3D Crystal Formation of 2,6-Bis[4-ethylphenyl]anthracene with Isotropic High Charge-Carrier Mobility, *Advanced Electronic Materials*, 2017,**3** ,1700282.
- [3] A. Li, L. Yan, M. Liu, I. Murtaza, C. He, D. Zhang, Y. He, H. Meng, Highly responsive phototransistors based on 2, 6-bis (4-methoxyphenyl) anthracene single crystal, *Journal of Materials Chemistry C*, 2017,**5** 5304-5309.